DNA Nanotechnology

Deutsche Ausgabe: DOI: 10.1002/ange.201502066
Internationale Ausgabe: DOI: 10.1002/anie.201502066

DNA-Grafted Supramolecular Polymers: Helical Ribbon Structures Formed by Self-Assembly of Pyrene–DNA Chimeric Oligomers**

*Yuliia Vyborna, Mykhailo Vybornyi, Alexander V. Rudnev, and Robert Häner**

Abstract: *The controlled arraying of DNA strands on adaptive polymeric platforms remains a challenge. Here, the noncovalent synthesis of DNA-grafted supramolecular polymers from short chimeric oligomers is presented. The oligomers are composed of an oligopyrenotide strand attached to the 5′-end of an oligodeoxynucleotide. The supramolecular polymerization of these oligomers in an aqueous medium leads to the formation of one-dimensional (1D) helical ribbon structures. Atomic force and transmission electron microscopy show rod-like polymers of several hundred nanometers in length. DNA-grafted polymers of the type described herein will serve as models for the development of structurally and functionally diverse supramolecular platforms with applications in materials science and diagnostics.*

DNA plays an important role in modern nanotechnology.[1–12] The merging of organic entities, such as polymers,[13] lipid chains,[14,15] or aromatic molecules[16–24] with DNA motifs enables the design and engineering of supramolecular architectures with special optical, mechanical, or biological properties.[25–30] While the self-assembly behavior of the resulting DNA conjugates is controlled by base-pairing interactions,[31] the overall structural and functional properties of the hybrid materials can be directed by the conjugated moieties.[32–35] In DNA-grafted polymers[36] (Scheme 1 A) oligonucleotides are arranged in a comb-like fashion on a polymer backbone. DNA polymer hybrids were shown to adopt morphologically well-defined shapes that are influenced by environmental factors.[37] Not surprisingly, such polymers find interest as materials with various applications, including drug delivery or DNA sensing,[38] and it is highly desirable to further enhance the functional diversity of both, the DNA and the polymer parts.[37,39–41] Supramolecular polymers are formed by noncovalent interactions[42,43] and thus bear additional responsiveness toward external stimuli in comparison to covalent polymers. In the present report, we describe the formation of DNA-grafted supramolecular polymers (Scheme 1 B). We show that pyrene–DNA chimeric oligomers self-assemble into ribbon-like helical structures in aqueous medium.

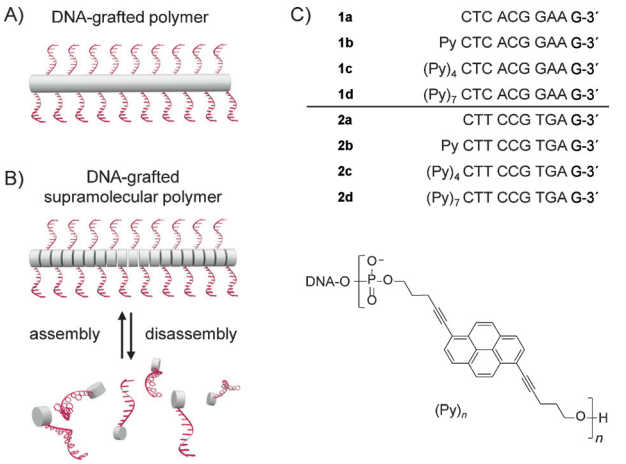

Scheme 1. Schematic representation of A) a DNA-grafted polymer and B) a DNA-grafted supramolecular polymer. C) DNA hybrid sequences used in this study and chemical structure of the phosphodiester-linked pyrene units.

The chimeric pyrene–DNA oligomers[44–46] used in this study were prepared by solid-phase synthesis following reported procedures[47] and are summarized in Scheme 1 C (see also the Supporting Information). The oligomers are composed of a DNA strand (10 nucleotides) and a 5′-linked pyrene part of variable length (0, 1, 4, or 7 units). Individual 1,6-bis-pentynyl pyrene units are linked by phosphodiester groups. The DNA sequences of series **1** and **2** are complementary.

All oligomers were found to be soluble at elevated temperatures (> 80 °C) in aqueous medium (100 mM NaCl, 10 mM sodium phosphate buffer, pH 7). The formation of polymers takes place upon slow cooling (0.1 °C min^{-1}) of a 2 μM solution of oligomers **1d** or **2d**. The polymerization process is conveniently followed by monitoring the UV/Vis absorption. The simultaneous formation of an H-band at 335 nm ($S_0 \rightarrow S_1$, Figure 1 A,B) and a J-band at 305 nm ($S_0 \rightarrow S_2$) is reminiscent of previous observations made with 1,6-linked pyrene oligomers and is explained by a stair-like folding of pyrene oligomers.[48,49] The stair-like folding of the seven pyrenes present in oligomers **1d** or **2d** is illustrated in Figure 1 C. The folded oligopyrenes consist of a layer of pyrenes that are flanked by the negative charges of the phosphodiester groups located on the edges of the stack. Subsequent aggregation of individual oligomers leads to the formation of supramolecular polymers.

Investigation of the samples after cooling to room temperature by atomic force microscopy (AFM) on an

[*] Y. Vyborna, M. Vybornyi, Dr. A. V. Rudnev, Prof. Dr. R. Häner
Department of Chemistry and Biochemistry, University of Bern
Freiestrasse 3, 3012 Bern (Switzerland)
E-mail: robert.haener@dcb.unibe.ch

[**] This work was supported by the Swiss National Foundation (Grant 200020_149148; R.H.) and FP7 Project ACMOL (Grant 618082; A.V.R.).

Supporting information for this article is available on the WWW under http://dx.doi.org/10.1002/anie.201502066.

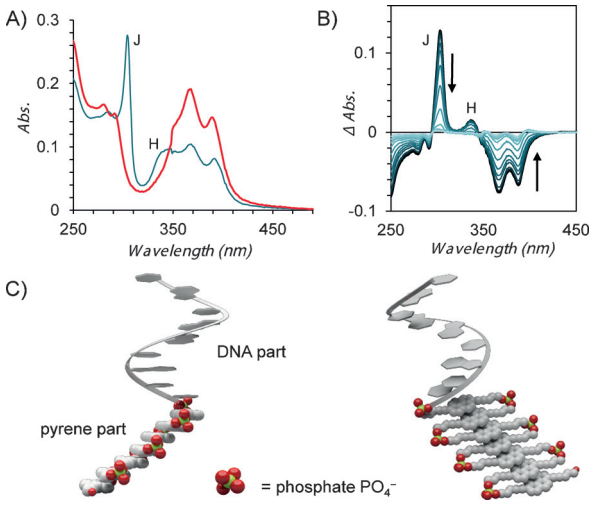

Figure 1. A) UV/Vis spectra of **1d** at 90 °C (red) and 20 °C (blue). B) Temperature-dependent changes (Δ *Abs.*) in the absorption spectra of **1d**; direction of arrows indicates increasing temperature (20 °C→90 °C; 10 °C intervals). Conditions: oligomer concentration 2 μM, 10 mM phosphate buffer, pH 7, 100 mM sodium chloride. C) Model for the pyrene–DNA chimeric oligomers used in the present study. Pyrene units are arranged in a stair-like fashion; negatively charged phosphodiester groups are located on the edges of the pyrene stack. The appended oligodeoxynucleotide is illustrated as a right-handed helix.

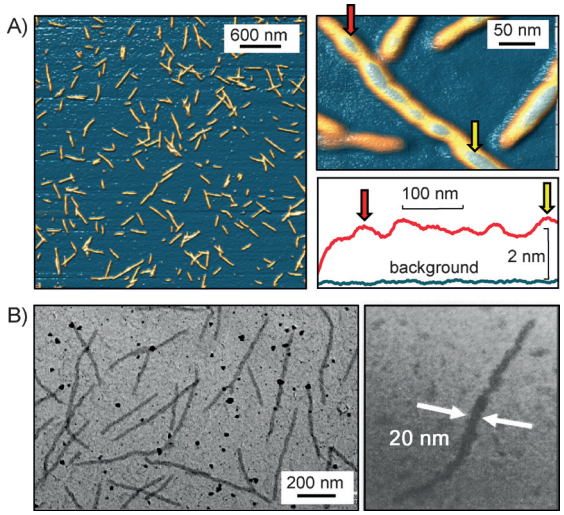

Figure 2. A) AFM images of supramolecular polymers formed from **1d** (left; 1 μM) and from a 1:1 mixture of **1d**/**2d** (top right; bottom: trace of polymer height profile). B) TEM images of polymers formed from **1d**/**2d**. Conditions: 10 mM phosphate buffer, pH 7, 250 mM sodium chloride; total strand concentration 10 μM unless indicated otherwise.

amino-modified mica surface shows the formed polymers (Figure 2A and Supporting Information). The polymers exhibit a one-dimensional (1D) shape. They appear as rod-like objects that are highly uniform with respect to their thickness (2.0 ± 0.2 nm). Their length considerably depends on the ionic strength. At 100 mM NaCl, the length ranges from 30–100 nm, and it reaches 300–500 nm upon increasing the NaCl concentration to 250 mM. Remarkably, the same type of polymers also forms from a solution containing a 1:1 mixture of oligomers **1d** and **2d**. This observation indicates that the interaction between the pyrene segments outweighs the base-pairing interactions between the complementary DNA strands. On the other hand, oligomers **1b**, **1c**, **2b**, and **2c**, which differ from **1d** and **2d** in the number of pyrene units present in the oligomer, did not lead to the formation of any elongated polymers (objects on a small nm scale are found for **1c** and **2c**) under the same conditions.

Interestingly, the 1D polymers formed from oligomers **1d** and/or **2d** exhibit an apparent helical structure. The helical pitch can be determined by tracking the thickness of the objects along their contour (Figure 2A). Statistical evaluation of the peak-to-valley profiles renders an average pitch value of 50 ± 15 nm (Supporting Information). Transmission electron microscopy (TEM) was used as an additional tool to visualize the DNA-grafted supramolecular polymers on surfaces (Figure 2B). The TEM images of the **1d**/**2d** self-assemblies provide further evidence that the aggregates exist as helical ribbons. The ribbons appear on a carbon-coated copper grid as 1D objects with a width of 19 ± 2 nm and a length of several hundred nanometers.

The polymerization process of **1d** and a 1:1 mixture of **1d**/**2d** was investigated in more detail by temperature-dependent UV/Vis studies. Figure 3 shows the degree of polymerization (α_{agg}) as monitored by the development of the J-band

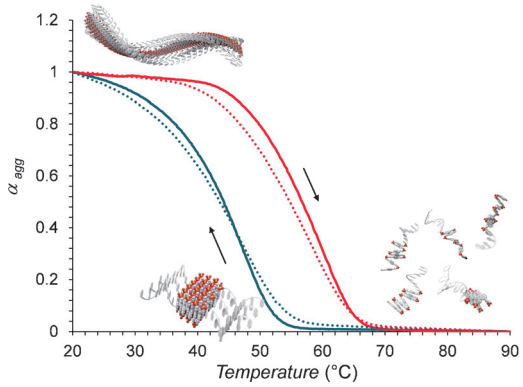

Figure 3. Heating (red) and cooling (blue) curves recorded with a solution of **1d** (dotted) or a 1:1 mixture of **1d**/**2d** (solid); direction of arrows indicates change of temperature. Conditions: see Figure 1; temperature gradient: 0.1 °C min^{-1}.

(305 nm). A substantial hysteresis is present (≈12 °C at $\alpha_{agg} = 0.5$) between melting and annealing curves. To minimize kinetic effects, the heating/cooling curves were recorded using a low temperature gradient (0.1 °C min^{-1}). The shapes of the curves for both, the single- and double-component systems, are similar and exhibit the typical features of a cooperative nucleation–elongation mechanism. The cooling curves were fitted to the described theoretical model.[50] The derived elongation temperature (T_e) is approximately 51 ± 1 °C for both systems under the employed conditions (see Supporting Information).

The proposed model for the formation of DNA-grafted supramolecular polymers by cooperative self-assembly is

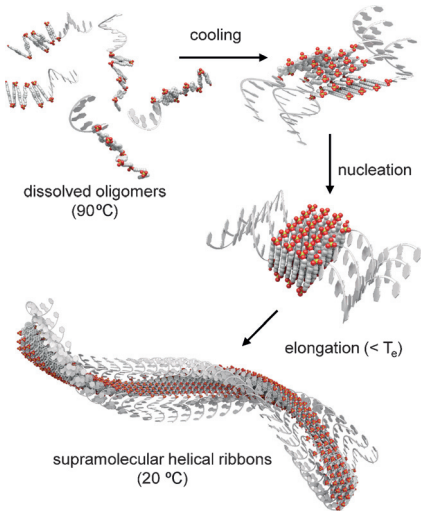

Scheme 2. Formation of DNA-grafted supramolecular polymers from chimeric DNA-pyrene oligomers through a nucleation–elongation process.

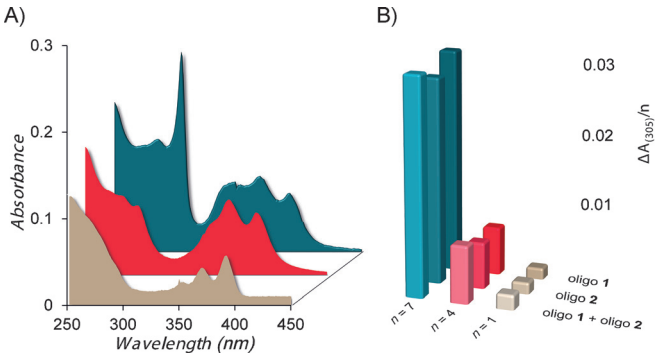

Figure 4. A) UV/Vis spectra of the binary mixtures **1b–d**/**2b–d** (brown **1b**/**2b**, red **1c**/**2c**, blue **1d**/**2d**) at 20 °C. B) changes in absorbance at 305 nm (J-band) per pyrene unit (*n*) upon cooling the oligomer solutions from 90 °C to 20 °C. Conditions: see Figure 1.

illustrated in Scheme 2. At elevated temperatures, oligomeric molecules (**1d** and/or **2d**) exist as molecularly dissolved chains. Upon cooling, the oligomers tend to self-assemble to form small aggregates. Assembly of individual strands is driven by hydrophobic and stacking interactions of pyrene residues. Further cooling leads to the formation of nuclei that serve as templates for the elongation of the polymers. Fitting of the curves according to the nucleation–elongation theory allows an estimation of the number (*N*) of oligomers needed to form the nuclei. For both types of systems, the number of oligomers required for the formation of a nucleus is approximately seven. The continued addition of oligomers to the nuclei occurs in a cooperative manner and leads to the formation of the helical ribbon structures. Importantly, nucleation occurs at temperatures that are considerably higher than the melting temperature (T_m) of the DNA hybrid formed of the two complementary oligodeoxynucleotides **1a**/**2a** ($T_m = 37$ °C, see the Supporting Information). Furthermore, spectroscopic and microscopic differences between single- and double-component mixtures (i.e. polymers formed from **1d** or **2d** alone or from a 1:1 mixture of both) are minor. This observation provides further strong evidence that the formation of the supramolecular polymers is largely driven by intermolecular interactions between the pyrene segments and interactions between the nucleotide segments, even canonical base pairing, play a minor role. On the other hand, the stability of the polymers is strongly dependent on the length of the pyrene stretch. When the number of pyrenes is reduced, such as in oligomers **1b**,**c** or **2b**,**c**, no polymers of comparable length or shape can be observed by microscopic methods. This is paralleled by UV/Vis data, as shown in Figure 4. Oligomers containing four instead of seven pyrenes exhibit only an ill-defined J-band upon decreasing the temperature from 90 °C to 20 °C. If only a single pyrene is appended to the oligonucleotide, the J-band is not observed at all.

Fluorescence spectroscopy provides additional information on the nature of the DNA-grafted supramolecular polymers. The fluorescence spectra of **1d**- and/or **2d**-derived 1D ribbons show a combination of pyrene monomer and excimer emission (see the Supporting Information). The pyrenes are confined in a rigid network of ladder-type folded oligomers. This reduces the probability of pyrenes to form excimers. Therefore, a relatively large part of the relaxation occurs through monomer emission, thus leading to monomer and excimer signals of comparable intensity for the polymers. In comparison, samples containing oligomers **1c** and/or **2c** do not form equally well-defined aggregates; the pyrenes are conformationally less restricted and exhibit predominantly excimer emission. Additionally, experiments with Cy5-labeled complementary strands show that energy transfer takes place from pyrene to the Cy5-acceptor dye[51] attached either to the 3′ or the 5′ end (see the Supporting Information, Figure S22). Energy transfer occurs in an efficient, distance-dependent way. This result confirms that the DNA strands are accessible for hybridization and retain their functionality.

The self-assembly of lipid-modified DNA has been intensively studied. Most morphological experiments show the formation of micelles or vesicles.[14,52–55] The controlled formation of one-dimensional DNA-grafted platforms is however rather unusual.[56–58] It is also noteworthy that the 1D shape of the polymers described here is in sharp contrast to the two-dimensional (2D) polymers formed by pyrene trimers.[38,39] The confinement of polymeric growth in one direction is explained by the presence of the oligonucleotide attached to one end of the oligopyrene strand. Supramolecular polymerization is driven by hydrophobic and stacking interactions between the pyrenes. Because of the presence of the negatively charged edges, growth of the polymers can take place only in a planar mode. The presence of the DNA strand represents a further delimitation and directs the addition of subsequent pyrene oligomers in a linear (or quasi-linear) fashion, as illustrated in Scheme 2. Because of repulsive forces between the negatively charged individual DNA strands, it can be reasonably assumed that the latter are positioned along either side of the ribbon-like pyrene polymer with more or less equal distribution.

In summary, we have described the preparation of DNA-grafted supramolecular polymers from short chimeric DNA–pyrene oligomers. Oligodeoxynucleotide strands are arranged along the edges of a ribbon-shaped helical aggregate of self-assembled pyrene segments with a helical pitch of approximately 50 nm. The length of the polymers can reach up to 500 nm and depends on the ionic strength of the medium. Hydrophobic and stacking interactions between intramolecularly folded pyrene chains are the major driving force for the polymerization, which occurs through a nucleation–elongation process. The type of DNA-grafted polymer described here may serve as a model for the development of structurally and functionally diverse supramolecular platforms with applications in materials science and diagnostics.

Keywords: DNA · nanotechnology · pyrene · self-assembly · supramolecular polymers

How to cite: *Angew. Chem. Int. Ed.* **2015**, *54*, 7934 – 7938
Angew. Chem. **2015**, *127*, 8045 – 8049

[1] M. Kwak, A. Herrmann, *Angew. Chem. Int. Ed.* **2010**, *49*, 8574 – 8587; *Angew. Chem.* **2010**, *122*, 8754 – 8768.
[2] K. M. M. Carneiro, N. Avakyan, H. F. Sleiman, *WIREs Nanomed. Nanobiotechnol.* **2013**, *5*, 266 – 285.
[3] A. Patwa, A. Gissot, I. Bestel, P. Barthélémy, *Chem. Soc. Rev.* **2011**, *40*, 5844 – 5854.
[4] D. Yang, M. J. Campolongo, T. N. Nhi Tran, R. C. H. Ruiz, J. S. Kahn, D. Luo, *WIREs Nanomed. Nanobiotechnol.* **2010**, *2*, 648 – 669.
[5] M. R. Jones, N. C. Seeman, C. Mirkin, *Science* **2015**, *347*, 1260901.
[6] T. Tørring, N. V. Voigt, J. Nangreave, H. Yan, K. V. Gothelf, *Chem. Soc. Rev.* **2011**, *40*, 5636 – 5646.
[7] J. Wengel, *Org. Biomol. Chem.* **2004**, *2*, 277 – 280.
[8] A. Heckel, M. Famulok, *Biochimie* **2008**, *90*, 1096 – 1107.
[9] M. Endo, H. Sugiyama, *ChemBioChem* **2009**, *10*, 2420 – 2443.
[10] H. Liang, X. B. Zhang, Y. Lv, L. Gong, R. Wang, X. Zhu, R. Yang, W. Tan, *Acc. Chem. Res.* **2014**, *47*, 1891 – 1901.
[11] F. Wang, X. Liu, I. Willner, *Angew. Chem. Int. Ed.* **2015**, *54*, 1098 – 1129; *Angew. Chem.* **2015**, *127*, 1112 – 1144.
[12] B. Saccà, C. M. Niemeyer, *Angew. Chem. Int. Ed.* **2012**, *51*, 58 – 66; *Angew. Chem.* **2012**, *124*, 60 – 69.
[13] F. E. Alemdaroglu, A. Herrmann, *Org. Biomol. Chem.* **2007**, *5*, 1311 – 1320.
[14] M. Schade, D. Berti, D. Huster, A. Herrmann, A. Arbuzova, *Adv. Colloid. Interface Sci.* **2014**, *208*, 235 – 251.
[15] U. Jakobsen, A. C. Simonsen, S. Vogel, *J. Am. Chem. Soc.* **2008**, *130*, 10462 – 10463.
[16] E. Stulz, *Chem. Eur. J.* **2012**, *18*, 4456 – 4469.
[17] Y. N. Teo, E. T. Kool, *Chem. Rev.* **2012**, *112*, 4221 – 4245.
[18] R. Varghese, H. A. Wagenknecht, *Chem. Commun.* **2009**, 2615 – 2624.
[19] V. L. Malinovskii, D. Wenger, R. Häner, *Chem. Soc. Rev.* **2010**, *39*, 410 – 422.
[20] C. Dohno, K. Nakatani, *Chem. Soc. Rev.* **2011**, *40*, 5718 – 5729.
[21] H. Kashida, X. Liang, H. Asanuma, *Curr. Org. Chem.* **2009**, *13*, 1065 – 1084.
[22] V. V. Filichev, E. B. Pedersen in *Wiley Encyclopedia of Chemical Biology*, *Vol. 1* (Ed.: T. P. Begley), Wiley, Hoboken, **2009**, pp. 493 – 524.
[23] M. E. Østergaard, P. J. Hrdlicka, *Chem. Soc. Rev.* **2011**, *40*, 5771 – 5788.
[24] A. Singh, M. Tolev, M. Meng, K. Klenin, O. Plietzsch, C. I. Schilling, T. Muller, M. Nieger, S. Braese, W. Wenzel, C. Richert, *Angew. Chem. Int. Ed.* **2011**, *50*, 3227 – 3231; *Angew. Chem.* **2011**, *123*, 3285 – 3289.
[25] D. Kedracki, I. Safir, N. Gour, K. X. Ngo, C. Vebert-Nardin, *Adv. Polym. Sci.* **2013**, *253*, 115 – 149.
[26] F. Pu, J. Ren, X. Qu, *Adv. Mater.* **2014**, *26*, 5742 – 5757.
[27] M. Langecker, V. Arnaut, T. G. Martin, J. List, S. Renner, M. Mayer, H. Dietz, F. C. Simmel, *Science* **2012**, *338*, 932 – 936.
[28] X. J. Chen, B. L. Sanchez-Gaytan, S. E. N. Hayik, M. Fryd, B. B. Wayland, S. J. Park, *Small* **2010**, *6*, 2256 – 2260.
[29] T. G. Edwardson, K. M. Carneiro, C. K. McLaughlin, C. J. Serpell, H. F. Sleiman, *Nat. Chem.* **2013**, *5*, 868 – 875.
[30] J. List, M. Weber, F. C. Simmel, *Angew. Chem. Int. Ed.* **2014**, *53*, 4236 – 4239; *Angew. Chem.* **2014**, *126*, 4321 – 4325.
[31] P. Beales, N. Geerts, K. K. Inampudi, H. Shigematsu, C. J. Wilson, T. K. Vanderlick, *J. Am. Chem. Soc.* **2013**, *135*, 3335 – 3358.
[32] A. C. Kamps, M. H. Cativo, X. J. Chen, S. J. Park, *Macromolecules* **2014**, *47*, 3720 – 3726.
[33] A. Ruiz-Carretero, P. G. Janssen, A. Kaeser, A. P. H. J. Schenning, *Chem. Commun.* **2011**, *47*, 4340 – 4347.
[34] P. P. Neelakandan, Z. Pan, M. Hariharan, Y. Zheng, H. Weissman, B. Rybtchinski, F. D. Lewis, *J. Am. Chem. Soc.* **2010**, *132*, 15808 – 15813.
[35] Z. Li, Y. Zhang, P. Fullhart, C. A. Mirkin, *Nano Lett.* **2004**, *4*, 1055 – 1058.
[36] M. Kwak, A. Herrmann, *Chem. Soc. Rev.* **2011**, *40*, 5745 – 5755.
[37] L. M. Randolph, M. P. Chien, N. C. Gianneschi, *Chem. Sci.* **2012**, *3*, 1363 – 1380.
[38] L. Peng, S. Wu, M. You, D. Han, Y. Chen, T. Fu, W. Tan, *Chem. Sci.* **2013**, *4*, 1928 – 1938.
[39] S. Averick, E. Paredes, W. Li, K. Matyjaszewski, S. R. Das, *Bioconjugate Chem.* **2011**, *22*, 2030 – 2037.
[40] K. Lee, J. M. Rouillard, T. Pham, E. Gulari, J. Kim, *Angew. Chem. Int. Ed.* **2007**, *46*, 4667 – 4670; *Angew. Chem.* **2007**, *119*, 4751 – 4754.
[41] J. M. Gibbs, S. J. Park, D. R. Anderson, K. J. Watson, C. A. Mirkin, S. T. Nguyen, *J. Am. Chem. Soc.* **2005**, *127*, 1170 – 1178.
[42] T. F. A. de Greef, M. M. J. Smulders, M. Wolffs, A. P. H. J. Schenning, R. P. Sijbesma, E. W. Meijer, *Chem. Rev.* **2009**, *109*, 5687 – 5754.
[43] T. Aida, E. Meijer, S. I. Stupp, *Science* **2012**, *335*, 813 – 817.
[44] R. Häner, F. Garo, D. Wenger, V. L. Malinovskii, *J. Am. Chem. Soc.* **2010**, *132*, 7466 – 7471.
[45] V. L. Malinovskii, A. L. Nussbaumer, R. Häner, *Angew. Chem. Int. Ed.* **2012**, *51*, 4905 – 4908; *Angew. Chem.* **2012**, *124*, 4989 – 4992.
[46] A. L. Nussbaumer, D. Studer, V. L. Malinovskii, R. Häner, *Angew. Chem. Int. Ed.* **2011**, *50*, 5490 – 5494; *Angew. Chem.* **2011**, *123*, 5604 – 5608.
[47] H. Bittermann, D. Siegemund, V. L. Malinovskii, R. Häner, *J. Am. Chem. Soc.* **2008**, *130*, 15285 – 15287.
[48] M. Vybornyi, A. Rudnev, R. Häner, *Chem. Mater.* **2015**, *27*, 1426 – 1431.
[49] M. Vybornyi, A. V. Rudnev, S. M. Langenegger, T. Wandlowski, G. Calzaferri, R. Häner, *Angew. Chem. Int. Ed.* **2013**, *52*, 11488 – 11493; *Angew. Chem.* **2013**, *125*, 11702 – 11707.
[50] P. Jonkheijm, P. van der Schoot, A. P. H. J. Schenning, E. W. Meijer, *Science* **2006**, *313*, 80 – 83.
[51] O. O. Adeyemi, V. L. Malinovskii, S. M. Biner, G. Calzaferri, R. Häner, *Chem. Commun.* **2012**, *48*, 9589 – 9591.
[52] G. Fuks, R. Mayap Talom, F. Gauffre, *Chem. Soc. Rev.* **2011**, *40*, 2475 – 2493.
[53] S. K. Albert, H. V. P. Thelu, M. Golla, N. Krishnan, S. Chaudhary, R. Varghese, *Angew. Chem. Int. Ed.* **2014**, *53*, 8492 – 8497; *Angew. Chem.* **2014**, *126*, 8632 – 8637.

[54] L. Tang, V. Tjong, N. Li, Y. G. Yingling, A. Chilkoti, S. Zauscher, *Adv. Mater.* **2014**, *26*, 3050 – 3054.
[55] Y. Dong, Y. Sun, L. Wang, D. Wang, T. Zhou, Z. Yang, Z. Chen, Q. Wang, Q. Fan, D. Liu, *Angew. Chem. Int. Ed.* **2014**, *53*, 2607 – 2610; *Angew. Chem.* **2014**, *126*, 2645 – 2648.
[56] L. Wang, Y. Feng, Z. Yang, Y. M. He, Q. H. Fan, D. Liu, *Chem. Commun.* **2012**, *48*, 3715 – 3717.
[57] M. P. Chien, A. M. Rush, M. P. Thompson, N. C. Gianneschi, *Angew. Chem. Int. Ed.* **2010**, *49*, 5076 – 5080; *Angew. Chem.* **2010**, *122*, 5202 – 5206.
[58] B. Waybrant, T. R. Pearce, E. Kokkoli, *Langmuir* **2014**, *30*, 7465 – 7474.

Received: March 4, 2015
Revised: March 31, 2015
Published online: May 8, 2015

